

Bi₂O₃ nanoparticles encapsulated in surface mounted metal–organic framework thin films†

Wei Guo,^a Zhi Chen,^b Chengwu Yang,^a Tobias Neumann,^b Christian Kübel,^{b,c} Wolfgang Wenzel,^b Alexander Welle,^{a,c} Wilhelm Pfleging,^{c,d} Osama Shekhah,^e Christof Wöll^a and Engelbert Redel^{*a}

We describe a novel procedure to fabricate a recyclable hybrid-photocatalyst based on Bi₂O₃@HKUST-1 MOF porous thin films. Bi₂O₃ nanoparticles (NPs) were synthesized within HKUST-1 (or Cu₃(BTC)₂) surface-mounted metal–organic frameworks (SURMOFs) and characterized using X-ray diffraction (XRD), a quartz crystal microbalance (QCM) and transmission electron microscopy (TEM). The Bi₂O₃ semiconductor NPs (diameter 1–3 nm)/SURMOF heterostructures exhibit superior photo-efficiencies compared to NPs synthesized using conventional routes, as demonstrated via the photodegradation of the nuclear fast red (NFR) dye.

Photocatalysts carry huge potential for the removal of contaminations from the environment and have been demonstrated to show an impressive performance in decomposing organic pollutants under UV-light irradiation.¹ Among the numerous semiconducting materials under investigation, recently, much attention has been given to Bi₂O₃ photocatalysts. Bi₂O₃ exhibits narrow electronic band gaps (2.8 eV or less) and shows p-type behavior with high photocatalytic activity.² Straightforward applications, however, are hampered by the fact that the fabrication of monodisperse Bi₂O₃ nanoparticles (NPs) with well defined-diameters represents a major challenge. Conventional NP synthesis methods typically yield rather broad NP size distributions.³ For the fabrication of high performance photocatalysts as well as for a more detailed understanding of the fundamental photocatalytic process, the development of a novel synthesis allowing the production of

Bi₂O₃ clusters and NPs with narrow size distributions and large surface areas is urgently required.

A very appealing strategy to attain this goal is the synthesis of NPs inside the voids of metal–organic frameworks (MOFs).⁴ Since the pore-walls of the MOF can be used to control the size of the NPs, as a result of their pore sizes and large loading capacity for guest species, this class of highly porous, crystalline materials provides an ideal platform for the encapsulation of catalytically active compounds (such as Pt,⁵ Au,⁶ Ti-based⁷) as well as of photosensitizers.⁸ MOFs are typically insulators, the size of the band-gap strongly depends on the nature of the organic ligands used to build the molecular frameworks.⁹ Over the past decade, an increasing number of studies have been reported using MOFs as a host matrix, which after loading with appropriate compounds act as a high-yield photocatalyst with a number of interesting properties, *e.g.* for hydrogen evolution (Pt@MOF),⁵ light-driven α -alkylation reactions (BCIP@MOF)¹⁰ and enantiomer recognition and separation in chiral MOC@SURMOF.¹¹

The present work is based on a particular MOF, HKUST-1, which is grown in the form of thin, monolithic coatings on modified Au substrates using liquid-phase epitaxy (LPE), yielding so-called SURMOFs, surface-mounted metal–organic frameworks. Liquid-phase epitaxy (LPE) is a quite attractive method for depositing MOFs in a layer-by-layer controlled fashion, yielding very homogeneous, highly oriented and crystalline MOF thin films. SURMOFs can be manufactured with thicknesses ranging from the nanometer up to the micrometer-regime, and they allow for straightforward characterization of their mechanical,¹² optical,¹³ photonic¹⁴ and optoelectronic¹⁵ as well as their magnetic,¹⁶ electrical¹⁷ and electrochemical¹⁸ properties. In addition, SURMOFs provide a direct path to the fabrication of MOF-based membranes,¹⁹ which is of profound interest also in the area of water purification.

Here, we use the pores within the HKUST-1 SURMOFs for the synthesis of Bi₂O₃ clusters/NPs, yielding a novel Bi₂O₃@HKUST-1 (or Cu₃(BTC)₂, BTC = 1,3,5-benzenetricarboxylic acid) hybrid-photocatalyst. The layer-by-layer strategy is used to fabricate this hybrid material. These final hybrid-photocata-

^aKarlsruhe Institute of Technology, Institute of Functional Interfaces (IFG), Hermann von Helmholtz Platz 1, 76344 Eggenstein Leopoldshafen, Germany. E mail: Engelbert.Redel@kit.edu

^bKarlsruhe Institute of Technology, Institute of Nanotechnology (INT), Hermann von Helmholtz Platz 1, 76344 Eggenstein Leopoldshafen, Germany

^cKarlsruhe Institute of Technology, Karlsruhe Nano Micro Facility (KNMF), Hermann von Helmholtz Platz 1, 76344 Eggenstein Leopoldshafen, Germany

^dKarlsruhe Institute of Technology, Institute of Advanced Materials (IAM), Hermann von Helmholtz Platz 1, 76344 Eggenstein Leopoldshafen, Germany

^eAdvanced Membranes and Porous Materials Center, King Abdulah University of Science and Technology, Kingdom of Saudi Arabia

† Electronic supplementary information (ESI) available. See DOI: 10.1039/c6nr00532b

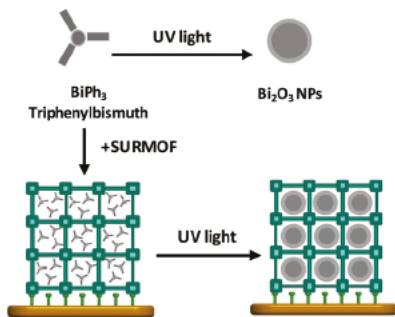


Fig. 1 Synthesis scheme of Bi_2O_3 @HKUST-1 SURMOFs.

lysts formed by our novel synthesis procedure consist of p-type Bi_2O_3 NPs embedded into HKUST-1 SURMOFs (Fig. 1). When the crystallite dimension of a semiconductor particle falls below a critical radius of approximately 10 nm, the charge carriers behave quantum mechanically, the band gap increases and the band edges shift to yield larger redox potentials.¹ Thus the use of quantum-sized Bi_2O_3 semiconductor NPs (1–3 nm) may result in increased photo-efficiencies for the systems in which the rate-limiting step is the charge transfer.

All HKUST-1 SURMOFs used in the present work were grown on modified Au substrates using the liquid-phase epitaxy (LPE) method, except parts of the TEM and UV-vis samples which were grown on quartz glass.²⁰ Surface modification was carried out by depositing a SAM (self-assembled monolayer) synthesized from 16-mercaptohexadecanoic acid (MHDA, 99%, Aldrich), and the SURMOFs were fabricated using a spray system, as described in detail in an earlier publication.²¹ The loading of BiPh_3 into the HKUST-1 SURMOFs was analyzed in a quantitative fashion using a quartz crystal microbalance (QCM) (Fig. S3†). The mass density of the activated framework amounts to 0.98 g cm^{-3} , which is increased by the ethanol contained in the pores, yielding a total mass-density of the ethanol-soaked HKUST-1 of 1.53 g cm^{-3} (see L. Heinke, Z. Gu and Ch. Woell, *Nat. Commun.*, 2014, 5, 4562 in the ESI†). Quantitative analysis of the QCM-data yields a BiPh_3 loading of $\sim 0.17 \text{ g BiPh}_3$ per g ethanol-soaked HKUST-1. This corresponds to a loading of 2–3 BiPh_3 molecules per HKUST-1 unit cell. After loading BiPh_3 , the reaction flask with a BiPh_3 @HKUST-1 sample was taken out from the oven and irradiated with 255 nm UV light for 5 h. Upon irradiation, the solution turns from clear to opaque (Fig. S4†). Subsequently, the sample was removed from the reaction solution, rinsed with pure ethanol and dried using dry N_2 gas. Then, the sample was irradiated with 255 nm UV light for 1 h.

The photocatalytic activity of these novel Bi_2O_3 @HKUST-1 SURMOFs was demonstrated using a commonly used test system, namely photoinduced decomposition of the NFR (Nuclear Fast Red, $\text{C}_{14}\text{H}_8\text{NO}_7\text{SNa}$) dye. A comparison with the activities of powder photocatalysts synthesized using conventional schemes, reveals a substantially increased activity. Since SURMOFs can also be used to fabricate membranes in a straightforward fashion,²² these monolithic, MOF-based thin

films are excellent candidates for the design and synthesis of highly active photocatalyst membranes e.g. in a flow-through fashion for UV-induced decomposition of organic pollutants from wastewater.

According to previous reports, the reactive Bi species formed by the photodecomposition of BiPh_3 in solution will, in the presence of O_2 , form Bi_2O_3 particles.²³ A similar reaction takes place in the pores of the MOF used in the present experiments, as confirmed by XPS-data, which after UV-exposure shows a characteristic Bi $4f_{5/2}$ peak with a binding energy at 167.1 eV (Fig. S5†). This describes the successful UV-decomposition of the BiPh_3 precursor molecule into Bi_2O_3 NPs. The XRD-data (Fig. 2b) reveal that the crystallinity of the MOF host lattice is not affected by the reaction. UV-Vis measurements (Fig. S6a†) demonstrate the presence of a semiconducting material with a bandgap of 2.7 eV, similar to that reported previously for Bi_2O_3 particles.²⁴ In Fig. 2b, we present the XRD data recorded in an out-of-plane geometry for the pristine, monolithic and oriented HKUST-1 SURMOF thin film (black). As reported in previous studies,²¹ the (002) and (004) peaks are well-defined and sharp, and their relative intensities are in full agreement with simulations assuming a perfect HKUST-1 material (Fig. 2b, black). The absence of diffraction peaks for the other crystallographic directions in the out-of-plane data reveals that the SURMOF growth proceeds only along the (001) crystallographic direction. The XRD data recorded after immersion of the HKUST-1 thin film into the BiPh_3 solution (Fig. 2b, red) reveal that loading the guest molecules does not affect the crystallinity of the host matrix. Although no new diffraction peaks appear, after loading, the ratio of the diffraction peak intensities is different. The (002)/(004) (out-of-plane data) ratio has decreased from 2.13 for the pristine film to 0.79 for the BiPh_3 loaded film. Longer immersion times did not lead to a further change of the relative XRD peak intensities. This change of form factors confirms that host molecules are loaded in virtually every pore of the MOF, e.g. a decoration of only the outer surface can be excluded

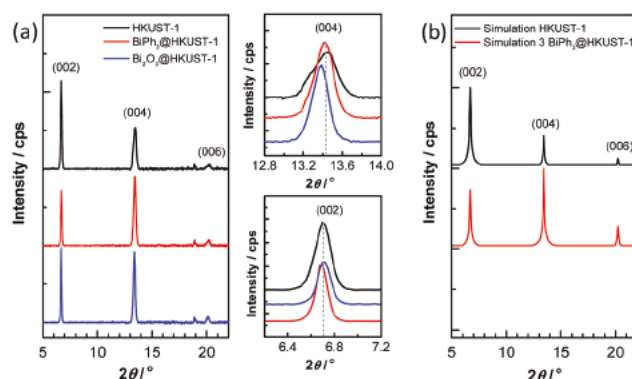


Fig. 2 X ray diffraction patterns recorded: (a) calculated XRD pattern for HKUST-1 [empty HKUST-1 (black) and after loading 3 BiPh_3 (red)] and (b) experimental XRD data recorded in the out of plane [empty HKUST-1 (black), after loading BiPh_3 (red), and after UV light irradiation (blue)] scattering geometry.

from such thin coating and it would not lead to a change of the XRD form factors.

We further suggest a model where 3 BiPh₃ are uniformly loaded within the HKUST-1 pores (Fig. S8a†). Force-field based simulations have been carried out to obtain the precise position of BiPh₃ molecules in the HKUST-1 lattice, as reported previously for other molecular guests in HKUST-1.²⁵ The best agreement of the XRD-data simulated for the different structures with the experimental XRD is obtained for 3 BiPh₃ molecules per HKUST-1 unit cell (Fig. 2a, red) which is also consistent with the QCM-data. We now turn our attention to the UV-induced nanoparticle synthesis inside the MOF pores. After the photoreduction, the XRD-data reveal a small shift to smaller diffraction angles, indicating a very slight (0.24%) expansion of the HKUST-1 unit cell. The (002)/(004) intensity ratio only shows a fairly small change, a slight increase from 0.79 to 1.05 (Fig. 2b, blue). Since the intensity ratio is clearly different from that seen for the empty HKUST-1, a pronounced sintering leading to the formation of large clusters embedded in the metal-organic framework can be excluded. Note that the maximum size of the (Bi₂O₃)_n NPs as judged from the TEM-data (observed diameters: 1–3 nm) is slightly larger than the size of the pores within the HKUST-1 (~1.9 nm). We explain this finding by the fact that during growth the BTC-ligands defining the walls of the MOF-pores are slightly displaced. This is similar to the formation of large Pd-clusters after the liberation of Pd from [(tmeda)Pd(CH₃)₂] (tmeda = *N,N,N',N'*-tetramethyl-ethylenediamine) as reported by Fischer and coworkers.²⁶

In order to further characterize the NP@MOF hybrid material, we have carried out investigations using Transmission Electron Microscopy (TEM) and Scanning Electron Microscopy (SEM). In this context, it should be noted that SURMOFs are particularly well suited for TEM and SEM investigations since they can be detached from the substrate, yielding flakes with a well-defined thickness and orientation. The HAADF-STEM data shown in Fig. 3a reveal the presence of Bi₂O₃ NPs with sizes of 1–3 nm distributed very uniformly within the HKUST-1.

The SAED (small area electron diffraction) data (Fig. 3b) shows a well-defined diffraction pattern which is fully consistent with the (111) orientation XRD diffraction data (SURMOF was grown on quartz glass facing the (111) orientation). HR-TEM diffraction patterns are further discussed in Table S1 of the ESI.† After photoreduction in the presence of O₂, we propose that (Bi₂O₃)_n clusters are formed. Since the TEM images show a sharp, but not a completely uniform size distribution, we conclude that during the photoinduced cluster formation Bi-containing species can diffuse into neighboring pores to form larger clusters.

Previous theoretical work has shown that various stoichiometric and neutral, closed-shell (Bi₂O₃)_n clusters with *n* = 1–5 clusters are stable.²⁷ Such (Bi₂O₃)_n NPs of different sizes are schematically depicted in Fig. S8b.† The presence of small (Bi₂O₃)_n NPs is also demonstrated by ToF-SIMS measurements carried out for the loaded HKUST-1 thin film, where BiO⁺, Bi₂O₂⁺, Bi₃O₄⁺, Bi₂O⁺ and other cationic oxide-cluster species

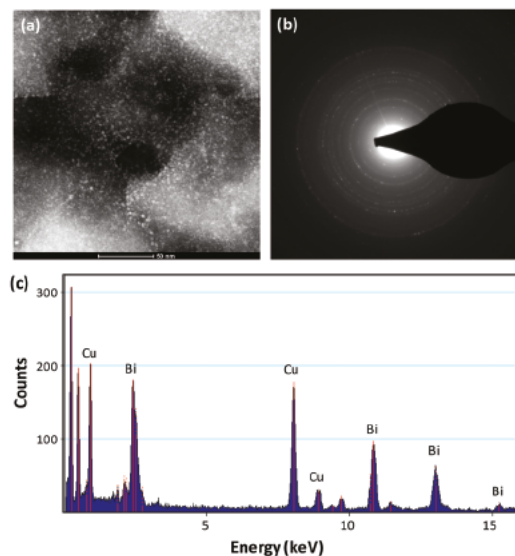


Fig. 3 (a) HAADF STEM images of Bi₂O₃@HKUST 1 SURMOFs. (b) SAED (Selected Area Electron Diffraction) patterns the Bi₂O₃@HKUST 1 SURMOFs. (c) Example EDX analysis of Bi₂O₃@HKUST 1 SURMOFs.

are detected (Fig. S9–S11†). Stable and closed shell cationic bismuth oxide clusters with the general formula (Bi₂O₃)_nBiO⁺ (*1* < *n* < 4) have been reported in previous studies.²⁸ Although some exchange of small species (particles with diameters smaller than the channel width in HKUST-1 MOFs of about 1.2 nm) between adjacent pores within the MOF is possible, a sintering of larger particles formed in the reaction can be ruled out. According to the TEM-data, (Bi₂O₃)_n-NPs have sizes between 1 nm and 3 nm (Fig. 3a and S1b of the ESI†). Our results thus demonstrate that pores within MOFs offer a unique opportunity for the synthesis of NPs with small size distributions. Clearly, after synthesizing Bi₂O₃ within the HKUST-1 SURMOF, an absorption change was observed in the range of 300–700 nm. Further results of the UV-vis measurements are shown in Fig. S6a of the ESI.† Furthermore, other metal-organic molecular precursors have been successfully loaded into MOFs, e.g. ferrocene²⁹ or Eu(bzac)₃bipy (bzac = 1-benzoylacetone, bipy = 2,2'-bipyridine).³⁰

The photocatalytic activity of Bi₂O₃@HKUST-1 was demonstrated using a standard test reaction, the degradation of a common dye, nuclear fast red (NFR). In order to determine the catalyst activity, we prepared a solution of NFR and then immersed the NP-loaded SURMOFs into the corresponding container. The concentration of the NFR dye was determined by measuring the absorbance at λ_{max} = 557 nm (Fig. 4c). As shown in Fig. 4b, five cases, pristine solution [40 μM water/EtOH (1 : 3) NFR solution], Au wafer (4 cm²), HKUST-1 (~6 μg cm⁻², 4 cm², mass ~ 24 μg), Bi₂O₃ (mass ~ 30 μg) and Bi₂O₃@HKUST-1 (~7 μg cm⁻², 4 cm², mass ~ 28 μg) immersed in 30 mL solution of the dye (40 μM), were studied. The decrease of the absorption conveniently allows us to study the adsorption of the NFR dye on the surface of the powder Bi₂O₃ particles and their diffusion into the empty and the Bi₂O₃ NP

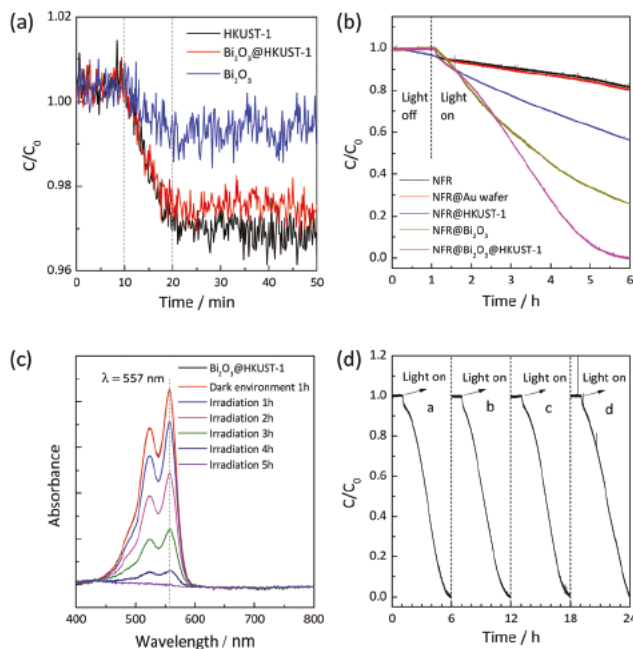


Fig. 4 (a) The absorption of the NFR dye in the HKUST 1 SURMOF (black), Bi_2O_3 @HKUST 1 SURMOF (magenta) and powder Bi_2O_3 (blue). (b) Photodegradation under different catalytic conditions [empty (black), Bi_2O_3 @HKUST 1 SURMOF (red), HKUST 1 SURMOF (blue), powder Bi_2O_3 (dark yellow) and gold wafer (red)] under UV light irradiation. (c) UV Vis absorption spectra of the NFR dye irradiated for different times with the Bi_2O_3 @HKUST 1 photocatalyst. (d) Four repeated processes of using the Bi_2O_3 @HKUST 1 photocatalyst for photodegradation of NFR under UV light irradiation.

loaded SURMOFs. This information is highly relevant of course for the Bi_2O_3 NPs encapsulated in the MOF to be photocatalytically active for NFR decomposition, where the NFR molecules should be able to diffuse inside the MOF lattice. The corresponding adsorption values as determined from the reduction of the absorption in the liquid are shown in Fig. 4a and amount to 3.2% (NFR dye mass ratio in solution) for the empty MOF and 2.6% for the NP loaded SURMOF. The adsorption on the powder material only amounted to 0.7%. Quantitative analysis of the decrease of 3% yields a loading of *ca.* 1–2 NFR dye molecules per MOF pore. After loading the Bi_2O_3 NPs, the value is slightly decreased, indicating that the diffusivity of the NFR molecules inside the MOF is essentially unaffected by the loaded Bi_2O_3 NPs. After about one hour, the concentration of the NFR molecules in the solution reached a stable concentration and no further reduction of the absorption was observed, demonstrating that no decomposition of the NFR dye took place in the dark. When UV-light (255 nm) was turned on, a gradual reduction of the NFR-concentration was observed, directly demonstrating the photocatalytic decomposition of the NFR dye molecules. The corresponding concentrations as a function of time are presented in Fig. 4b. In the next step experiments, the solutions were exposed to 255 nm UV light. 100% degradation of NFR was achieved in the presence of the Bi_2O_3 @HKUST-1 thin film within 5 hours.

This result clearly indicates that the photodegradation of Bi_2O_3 @HKUST-1 thin film samples is the most efficient. Reference experiments for the pure HKUST-1 and (non-encapsulated) Bi_2O_3 yielded a degradation of 44% and 74% degradation of NFR under the same conditions, respectively.

These results demonstrate that a NP@MOF system exhibits significant photochemical activity for the degradation of the NFR dye which is larger than that of the individual components. This higher activity of the NP@MOF hybrid material to the individual components can be explained through the higher surface area of the NP@MOF hybrid material. The pore in the HKUST-1 MOF leads to stabilization of the small Bi_2O_3 clusters/NPs and avoids any sintering/clustering of individual NPs. Furthermore, we speculate that an efficient charge-separation process takes place in the Bi_2O_3 @HKUST-1 hybrid material, similar to already published work on QD@MOF systems.^{31a,b} The regeneration and reusability of Bi_2O_3 @HKUST-1 were investigated by repeating the NFR degradation at least four times. The photocatalyst was immersed in fresh NFR solutions and exposed to UV irradiation for 1 h. As shown in Fig. 4d, no deactivation of the photocatalyst is observed after four consecutive runs. XRD characterization carried out after these experiments showed no significant changes (Fig. S12†). Both observations suggest that the NP@SURMOF photocatalysts are stable, and no decomposition or structural changes are absorbed after the NFR dye photo-degradation (Fig. S13†). In addition, we have carried out measurements using Electro spray ionization mass spectrometry (ESI-MS) for the degraded solution (Fig. S14b†). The results allow for identifying six intermediate species (Fig. S14a†) generated in the course of NFR photodegradation. Based on the intermediates identified, a possible degradation pathway of the NFR dye is proposed, for details see Fig. S14a.†

Conclusions

We report a novel synthesis strategy to fabricate an efficient and recyclable, hybrid-photocatalyst. Such hybrid-photocatalysts are prepared using a Bi_2O_3 @HKUST-1 system by photodecomposition of BiPh_3 loaded into the pores of a metal-organic framework, yielding Bi_2O_3 -particles of a rather uniform size distribution, encapsulated into the pores of the MOF. This quantum-sized Bi_2O_3 semiconductor NPs (1–3 nm) in the HKUST-1 are expected to show increased photo-efficiencies for the systems in which the rate-limiting step is the charge transfer. The hybrid Bi_2O_3 @HKUST-1 SURMOF photocatalyst can be easily separated and recycled and it shows no significant loss in its photocatalytic activity. We further foresee a bright future for such hybrid-materials in the clean-tech field, *e.g.* as photocatalytic membrane compounds or in the field of sensors and catalysis.

Acknowledgements

Financial support by the Deutsche Forschungsgemeinschaft (DFG) within the Priority Program Metal Organic Frameworks

(SPP 1362) is gratefully acknowledged. E.R. thanks Landesstiftung Baden-Württemberg, KIT and CMM for sustainable research funding. We further thank Prof. Feldmann for providing us with precursor molecules. The support from the KNMF Laboratory for Microscopy and Spectroscopy and laser processing (<http://www.knmf.kit.edu>) is gratefully acknowledged. The authors further acknowledge the financial support of the Chinese Scholarship Council (CSC).

Notes and references

- 1 D. Ravelli, D. Dondi, M. Fagnoni and A. Albini, *Chem. Soc. Rev.*, 2009, **38**, 1999.
- 2 D. N. Ke, T. Y. Peng, L. Ma, P. Cai and P. Jiang, *Appl. Catal., A*, 2008, **350**, 111.
- 3 K. Bogusz, M. Tehei, C. Stewart, M. McDonald, D. Cardillo, M. Lerch, S. Corde, A. Rosenfeld, H. K. Liu and K. Konstantinov, *RSC Adv.*, 2014, **4**, 24412.
- 4 (a) H. Li, M. Eddaoudi, M. O'Keeffe and O. M. Yaghi, *Nature*, 1999, **402**, 276; (b) R. Makiura, S. Motoyama, Y. Umemura, H. Yamanaka, O. Sakata and H. Kitagawa, *Nat. Mater.*, 2010, **9**, 565.
- 5 C. Wang, K. E. de Krafft and W. B. Lin, *J. Am. Chem. Soc.*, 2012, **134**, 7211.
- 6 H. L. Jiang, B. Liu, T. Akita, M. Haruta, H. Sakurai and Q. Xu, *J. Am. Chem. Soc.*, 2009, **131**, 11302.
- 7 J. K. Gao, J. W. Miao, P. Z. Li, W. Y. Teng, L. Yang, Y. L. Zhao, B. Liu and Q. C. Zhang, *Chem. Commun.*, 2014, **50**, 3786.
- 8 S. Pullen, H. H. Fei, A. Orthaber, S. M. Cohen and S. Ott, *J. Am. Chem. Soc.*, 2013, **135**, 16997.
- 9 V. Stavila, A. A. Talin and M. D. Allendorf, *Chem. Soc. Rev.*, 2014, **43**, 5994.
- 10 P. Y. Wu, C. He, J. Wang, X. J. Peng, X. Z. Li, Y. L. An and C. Y. Duan, *J. Am. Chem. Soc.*, 2012, **134**, 14991.
- 11 Z. G. Gu, H. Fu, T. Neumann, Z. X. Xu, W. Q. Fu, W. Wenzel, L. Zhang, J. Zhang and C. Wöll, *ACS Nano*, 2016, **10**, 977–983.
- 12 S. Bundschuh, O. Kraft, H. K. Arslan, H. Gliemann, P. G. Weidler and C. Wöll, *Appl. Phys. Lett.*, 2012, 101.
- 13 E. Redel, Z. B. Wang, S. Walheim, J. X. Liu, H. Gliemann and C. Wöll, *Appl. Phys. Lett.*, 2013, 103.
- 14 J. X. Liu, E. Redel, S. Walheim, Z. B. Wang, V. Oberst, J. X. Liu, S. Heissler, A. Welle, M. Moosmann, T. Scherer, M. Bruns, H. Gliemann and C. Wöll, *Chem. Mater.*, 2015, **27**, 1991.
- 15 J. X. Liu, W. C. Zhou, S. Walheim, Z. B. Wang, P. Lindemann, S. Heissler, J. X. Liu, P. G. Weidler, T. Schimmel, C. Wöll and E. Redel, *Opt. Express*, 2015, **23**, 13725.
- 16 M. E. Silvestre, M. Franzreb, P. G. Weidler, O. Shekhah and C. Wöll, *Adv. Funct. Mater.*, 2013, **23**, 1210.
- 17 A. A. Talin, A. Centrone, A. C. Ford, M. E. Foster, V. Stavila, P. Haney, R. A. Kinney, V. Szalai, F. El Gabaly, H. P. Yoon, F. Leonard and M. D. Allendorf, *Science*, 2014, **343**, 66.
- 18 A. Dragasser, O. Shekhah, O. Zybaylo, C. Shen, M. Buck, C. Wöll and D. Schlettwein, *Chem. Commun.*, 2012, **48**, 663.
- 19 O. Shekhah, J. X. Liu, R. A. Fischer and C. Wöll, *Chem. Soc. Rev.*, 2011, **40**, 1081.
- 20 H. K. Arslan, O. Shekhah, J. Wohlgemuth, M. Franzreb, R. A. Fischer and C. Wöll, *Adv. Funct. Mater.*, 2011, **21**, 422.
- 21 H. K. Arslan, O. Shekhah, D. C. F. Wieland, M. Paulus, C. Sternemann, M. A. Schroer, S. Tiemeyer, M. Tolan, R. A. Fischer and C. Wöll, *J. Am. Chem. Soc.*, 2011, **133**, 8158.
- 22 P. Lindemann, M. Tsotsalas, S. Shishatskiy, V. Abetz, P. Krolla-Sidenstein, C. Azucena, L. Monnereau, A. Beyer, A. Golzhauser, V. Mugnaini, H. Gliemann, S. Brase and C. Wöll, *Chem. Mater.*, 2014, **26**, 7189.
- 23 R. J. F. Berger, D. Rettenwander, S. Spirk, C. Wolf, M. Patzschke, M. Ertl, U. Monkowius and N. W. Mitzel, *Phys. Chem. Chem. Phys.*, 2012, **14**, 15520.
- 24 L. S. Zhang, W. Z. Wang, J. O. Yang, Z. G. Chen, W. Q. Zhang, L. Zhou and S. W. Liu, *Appl. Catal., A*, 2006, **308**, 105.
- 25 W. Guo, J. X. Liu, P. G. Weidler, J. X. Liu, T. Neumann, D. Danilov, W. Wenzel, C. Feldmann and C. Wöll, *Phys. Chem. Chem. Phys.*, 2014, **16**, 17918.
- 26 T. Steinke, C. Gemel, M. Winter and R. A. Fischer, *Angew. Chem., Int. Ed.*, 2002, **41**, 4761.
- 27 G. Geudtner, P. Calaminici and A. M. Koster, *J. Phys. Chem. C*, 2013, **117**, 13210.
- 28 A. Fiellicke and K. Rademann, *J. Phys. Chem. A*, 2000, **104**, 6979.
- 29 W. C. Zhou, C. Wöll and L. Heinke, *Materials*, 2015, **8**, 3767.
- 30 H. C. Streit, M. Adlung, O. Shekhah, X. Stammer, H. K. Arslan, O. Zybaylo, T. Ladnorg, H. Gliemann, M. Franzreb, C. Wöll and C. Wickleder, *ChemPhysChem*, 2012, **13**, 2699.
- 31 (a) L. J. Shen, S. J. Liang, W. M. Wu, R. W. Liang and L. Wu, *J. Mater. Chem. A*, 2013, **1**, 11473; (b) J. Aguilera-Sigalat and D. Bradshaw, *Coord. Chem. Rev.*, 2016, **307**, 267.